High-power high-stability Q-switched green laser with intracavity frequency doubling of diode-pumped composite ceramic Nd:YAG laser*

Wang Yu-Ye(王与烨), Xu De-Gang(徐德刚), Liu Chang-Ming(刘长明), Wang Wei-Peng(王卫鹏), and Yao Jian-Quan(姚建铨)

Institute of Laser and Optoelectronics, College of Precision Instrument and Optoelectronics Engineering, Tianjin University, Tianjin 300072, China

Key Laboratory of Optoelectronics Information Science and Technology, Tianjin University, Ministry of Education, Tianjin 300072, China

(Received 13 February 2012; revised manuscript received 21 March 2012)

We successfully obtain high-average-power high-stability Q-switched green laser based on diode-side-pumped composite ceramic Nd:YAG in a straight plano-concave cavity. The temperature distribution in composite ceramic Nd:YAG crystal is numerically analyzed and compared with that of conventional Nd:YAG crystal. By use of a composite ceramic Nd:YAG rod and a type-II high gray track resistance KTP (HGTR-KTP) crystal, a green laser with an average output power of 165 W is obtained at a repetition rate of 25 kHz, with a diode-to-green optical conversion of 14.68%, and a pulse width of 162 ns. To the best of our knowledge, both the output power and optical-to-optical efficiency are the highest values for green laser systems with intracavity frequency doubling of this novel composite ceramic Nd:YAG laser to date. The power fluctuation at around 160 W is lower than 0.3% in 2.5 hours.

Keywords: high-average-power green laser, high stability, composite ceramic Nd:YAG rod

PACS: 42.55.Xi, 42.60.Lh, 42.70.Hj **DOI:** 10.1088/1674-1056/21/9/094212

1. Introduction

Diode-pumped solid-state (DPSS) green lasers with high average power and high repetition rate have been in demand for various applications. In the industrial field, high-power all-solid-state green laser source is more suitable than infrared (IR) lasers in marking, precision micro fabrication, and trimming due to its lower spot size limit and larger absorbance for most materials. It has also been applied widely for ocean exploration, laser probe, and underwater communication due to its lower absorption in water. A high-power green laser has also been used for medical treatment such as laser clinical photo-selective vaporization of the prostate,[1] and proliferative diabetic retinopathy.[2] For all these applications, there is a constant demand for high-stability high-power output.

At present, intracavity frequency doubling of the high-power DPSS laser operating at a wavelength of about 1 μm based on KTP or LBO crystal has been proven to be an effective method of generating a high-average-power high-repetition-rate green laser. Green lasers with an average power higher than 100 W have been reported based on intracavity frequency-doubled Q-switched Nd-doped lasers during the past two decades.[3−16] Considerable efforts have been made to improve the power scalability by employing complicated Z-shaped[3,7,11] and V-shaped[5,6,8,10] folded cavity configurations to enhance the pump intensity in frequency doubling crystal. Compared with the folded cavities, the compact straight cavity is still preferred to be used in industrial floor due to its simplicity and stability.[9,12−16] More recently, green laser with an average power of 180 W and a pulse duration of 70 ns was achieved with two side-pumped Nd:YAG laser heads in series using straight cavity structure.[14] The power fluctuation is around ±1.2% during 2.5 hours. However, two laser heads in the system not only make the system bulky and expensive but also increase the complex-

*Project supported by the National Natural Science Foundation of China (Grant Nos. 61107086, 61172010, and 61101058), the Science and Technology Committee of Tianjin, China (Grant No. 11JCYBJC01100), and the National High Technology Research and Development Program of China (Grant No. 2011AA010205).

†Corresponding author. E-mail: yuyewang@tju.edu.cn

© 2012 Chinese Physical Society and IOP Publishing Ltd

ity of the system as the laser heads must be precisely aligned to avoid the distortion of the output beam profile. Moreover, both the pump heads should be identical in geometry for the compensation of pump-power-induced thermal birefringence in the Nd:YAG rod.

Generally, the power scalability and stability of the green laser are hampered primarily by the pump-power-induced thermal effect and thermal perturbation in the conventional gain medium. In order to develop high-stability high-power green laser systems, composite ceramic Nd:YAG crystal as the laser medium attracts our interest.[15,17] Average power of 104 W in a straight cavity has been obtained using diode-side-pumped laser with a diode-to-green optical conversion efficiency of 10.9%. Aside from that absorption spectrum, emission spectrum, and fluorescence lifetime of a ceramic Nd:YAG are very similar to those of a single-crystal Nd:YAG, the ceramic medium has the merits of large size, high concentration, low cost, good thermal conductivity, and composite structure.[18] Therefore, the ceramic YAG is expected to be an excellent host material of the laser gain media. In addition, the frequency doubling crystal is another important component for the high-power high-stability green lasers. The KTP crystal is an excellent crystal for second harmonic generation (SHG) due to the large nonlinear coefficient and temperature bandwidth. However, the gray-tracking problem, which may lead to a photochromic effect at a threshold intensity of 80 MW/cm^2,[19] has been a lasting one of KTP and limits the lifetime of KTP crystal for a high-average-power second harmonic generation. In recent years, high gray-track resistance KTP (HGTR-KTP) crystals have been developed.

In this paper, the thermal distribution in transversally pumped composite ceramic Nd:YAG crystal was numerically simulated with finite element method (FEM). A 165-W green laser employing intracavity frequency doubling of a diode-side-pumped double Q-switched composite ceramic Nd:YAG has been experimentally realized in a straight plano-concave cavity. The pulse width of green laser was 162 ns at repetition rate of 25 kHz. The two synchronized acousto–optic (AO) modulators were placed orthogonally to turn off the very high pump gain for efficient Q-switching operation. Type-II phase-matched HGTR-KTP crystal was used as frequency doubling nonlinear material in order to overcome the gray-track problem. The diode-to-green optical conversion efficiency reached 14.68%. To the best of our knowledge, both the average output power and optical-to-optical conversion efficiency at 532 nm are the highest values obtained with intracavity frequency doubling of such novel composite ceramic Nd:YAG laser. The average power fluctuation at around 160 W was lower than 0.3% within 2.5 hours.

2. Experimental setup

Figure 1 shows the schematic of experimental setup. The laser consists of four parts: a pump head to couple the diode laser beam to the composite ceramic Nd:YAG rod (Japan: Baikowski), a HGTR-KTP nonlinear crystal (Liaocheng, China: Dong'e Leeke) for intracavity frequency doubling, two acousto–optic modulator (USA: NEOS), and a harmonic separator and a resonator.

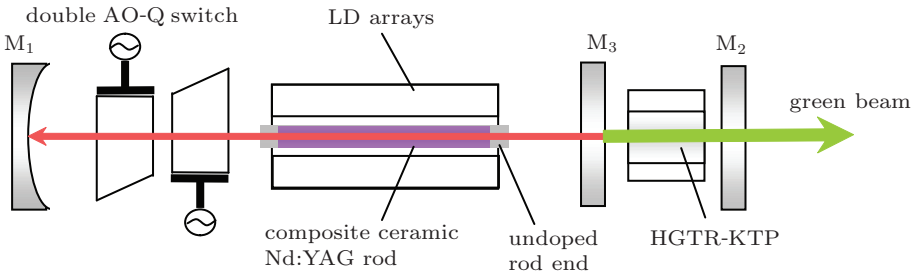


Fig. 1. (colour online) Schematic diagram of the green laser based on composite ceramic Nd:YAG crystal.

The optical pumping module consists of five laser diode (LD) stacked arrays (Cutting Edge Optronics), which were arranged in a pentagonal shape around the rod to achieve better pumping uniformity. Each stacked array consists of 16 laser diodes (808 nm wavelength, 20 W output power). The composite ceramic

Nd:YAG rod was mounted inside a flow tube whose outer surface was coated with an antireflective (AR) coating at the LD wavelength. The size of the rod was 6.35 mm in diameter and 144 mm in length. The 0.7 ± 0.02% Nd-doped middle part was 114 mm in length and side-polished, while undoped parts of the rod were about 15 mm long extended from both two ends. The end faces of the rod were polished and antireflection-coated at 1064 nm. Considering the thermal lens effect introduced by the Nd:YAG rod and the KTP crystal under high-power operation, we employed a plano-concave cavity structure in order to enhance the stability and efficiency. The total cavity length was 360 mm. The rear mirror M_1 was a concave mirror with curvature radius of 1 m and high reflectivity at 1.064 μm. Two synchronized acousto–optic modulators were placed orthogonally to fully switch off the high pump gain for efficient Q-switching operation. The repetition rate was optimized to be 25 kHz with respect to the green average power. The HGTR-KTP crystal with dimension of 6×6×10 mm^3, was antireflection-coated at 532 and 1064 nm, and it was placed between the flat output coupler M_2 (transmission is higher than 99.5% at 532 nm, reflection is higher than 99% at 1064 nm) and harmonic separator mirror M_3 (reflection is higher than 99.5% at 532 nm, transmission is higher than 98% at 1064 nm). The HGTR-KTP crystal not only has the merits of high nonlinear conversion coefficient, high temperature bandwidth, and small walking-off angle as fine as conventional KTP crystal, but also has higher damage threshold and it is suitable for high-power second harmonic generation. Moreover, it can overcome the gray-track problem. The KTP crystal used type-II phase matching type ($\theta = 90°$, $\varphi = 23.5°$) and was mounted inside 10-°C water to cool copper holder. Here, it should be pointed out that although the boundary temperature of KTP crystal can be kept constant in this way, the temperature in the middle of KTP crystal (the pumped volume) will still get higher as the 1064-nm pump power increases. Thus, the phase-matching condition is violated and the output green power is decreased. In order to compensate such thermal-induced phase mismatch, the incident angle to the KTP crystal should be adjusted to satisfy phase-matching condition.[20] Consequently, the phase-matching condition of type II KTP SHG can be fulfilled as pump power increases.

3. Theoretical simulation of temperature distribution

To study the advantage of the composite ceramic crystal and achieve high-stability laser output, we analyze the thermal distribution of the composite ceramic Nd:YAG. We consider an Nd:YAG rod that is transversely pumped and water cooled. Assuming the laser is under steady state, the temperature distribution $T(r, z)$ inside the laser rod can be described in the cylindrical coordinate system as

$$\frac{\partial^2 T}{\partial r^2} + \frac{1}{r}\frac{\partial T}{\partial r} + \frac{\partial^2 T}{\partial z^2} + \frac{Q}{k} = 0, \tag{1}$$

where k is the heat conductivity of the material and can be treated as a constant, and Q is the heat generated from the pump power per unit volume. Assuming a homogeneous pumping distribution in the laser crystal, Q is given by

$$Q = \frac{\eta_{\rm h} P_{\rm in}}{\pi r_0^2 L}, \tag{2}$$

where r_0 is the radius of the laser rod, $\eta_{\rm h}$ is the fraction of pump power converted to heat, $P_{\rm in}$ is the pump power, and L is the real pumped length of laser rod. In the calculation, the values of $\eta_{\rm h} = 0.42$,[21] $k = 13$ W/(m·K), $P_{\rm in} = 1124$ W, and $r_0 = 3.175$ mm were used.

The heat flow through the surface of the rod defines the boundary conditions, which is given by Newton's law of heat transfer[22]

$$k\frac{\partial T}{\partial n}\bigg|_{\rm Surf} = h(T_{\rm coolant} - T_{\rm Surf}), \tag{3}$$

where $T_{\rm coolant}$ is the coolant temperature which is taken as constant of surround cooling temperature, $T_{\rm Surf}$ is the local temperature on the surface, n is the local normal to that surface, and h is the heat transfer coefficient between coolant and rod surface. The surface of each rod end is in contact with air ($h_1 = 50$ W/(m^2·K)), and the remaining surface is water-cooled ($h_2 = 20000$ W/(m^2·K)). Both the temperature of the water coolant and air are set to be $T_{\rm coolant} = 23$ °C. In addition, as the convection coefficient of the composite crystal is much higher than that of the surface exposed to air, the thermal boundary condition at the interfaces of undoped and doped crystals are supposed to be adiabatic.

The temperature distribution in composite ceramic Nd:YAG crystal was numerically calculated using FE modeling, as shown in Fig. 2(a). The rod center is treated as the origin of the coordinate system due to the symmetry. Under the same condition, we

also calculated a conventional Nd:YAG crystal with dimension of $\Phi 6.35\times 114$ mm^2 to compare with the composite ceramic laser crystal, as shown in Fig. 2(b). As can be seen from the figures, the highest temperatures for the two kinds of crystals occurring at the center are the same and both of them increase to exceed the cooling water temperature of 71 K. However, the heat transfer along the axial axis is obvious for the ceramic Nd:YAG rod due to the undoped end, and the minimum temperature around the rod end is almost the same to coolant temperature. Figure 3 shows the temperature changes along the axial axis ($r = 0$) for two kinds of crystals. The arrows in Fig. 3 indicate the starting points from which the temperature decreases along both sides of the rod to the end. Taking half of the crystal as example ($r \geq 0$), for composite ceramic Nd:YAG crystal, the temperature gradually decreases from 367.6 to 296.3 K in the range of $21 < z < 72$ mm, whereas the temperature for conventional Nd:YAG crystal decreases from 367.6 to 367 K in the range of $31 < z < 57$ mm. Comparing the two cases, we note that the undoped ends designed for composite ceramic Nd:YAG laser can provide virtually uninhibited heat flow from doped to undoped region. The heat inside the crystal can be more effectively transfered to the outside. Therefore, the thermal tensile stress inside the laser rod can be efficiently reduced. This leads to almost no end thermal stress effect and thermal deformation, which can be a good method for stabilizing the optical power output.

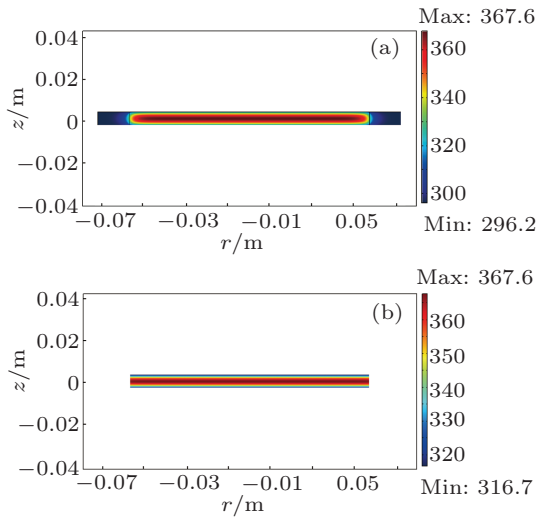


Fig. 2. (colour online) Thermal distribution in (a) composite ceramic Nd:YAG crystal and (b) conventional Nd:YAG crystal.

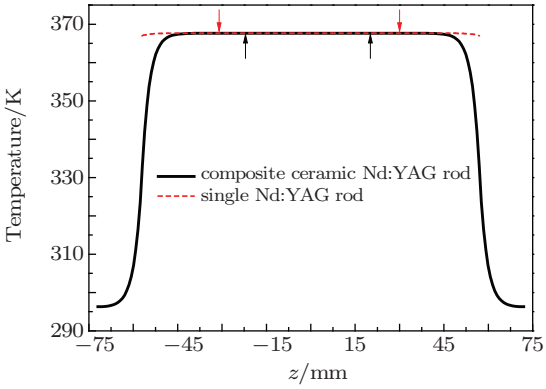


Fig. 3. (colour online) Thermal distribution along the axial axis for two kinds of crystals ($r = 0$).

4. Results and discussion

Figure 4 shows the average output power of the green laser and optical-to-optical conversion efficiency of the system as functions of the diode pump power when the repetition rate was 25 kHz. The solid squares denote the average power and the open circles denote the corresponding diode-to-green optical conversion efficiency. From Fig. 4, we can see that 532-nm average output power and optical-to-optical conversion efficiency increase with the diode pump power generally. The drop of the conversion efficiency after 1082 W is caused by the power saturation, because the resonator starts to operate at the edge of stable region as a result of thermal lensing effect. When the pump power is 1124 W, the maximum average output power of the green laser is 165 W with the optical-to-optical efficiency of 14.68%. To the best of our knowledge, both the green output power and efficiency are the highest values obtained by intracavity frequency doubling of this novel composite ceramic Nd:YAG laser. To characterize the pumping Nd:YAG laser, we measured the pump power of 1064-nm laser in the same cavity without KTP crystal and second harmonic mirrors, a 359-W 1064-nm continuous wave laser was obtained with transmission of 10% and pump power of 1124 W. In addition, we do not see any evidence of gray tracking in the HGTR-KTP crystals during our experiments. It confirms that the composite ceramic Nd:YAG rod and HGTR-KTP have excellent characteristics, and they can offer better laser performance and output stability even in the large pumping power range.

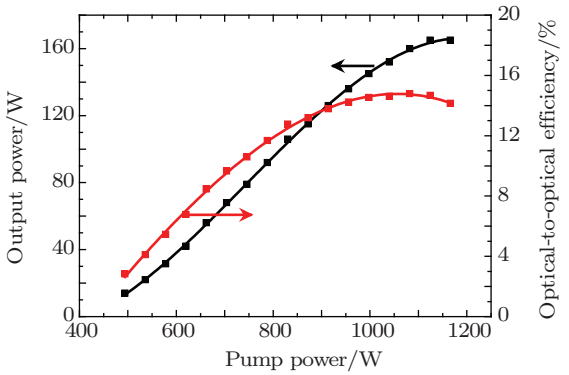


Fig. 4. (colour online) Output power of green laser and diode-to-green optical conversion efficiency as functions of the pump power.

Figure 5 shows the pulse shape at an average green output power of 165 W with a fast photodetector and the pulse train with a repetition rate of 25 kHz. The measured pulse width is 162.2 ns. The calculated pulse peak power is about 40.7 kW.

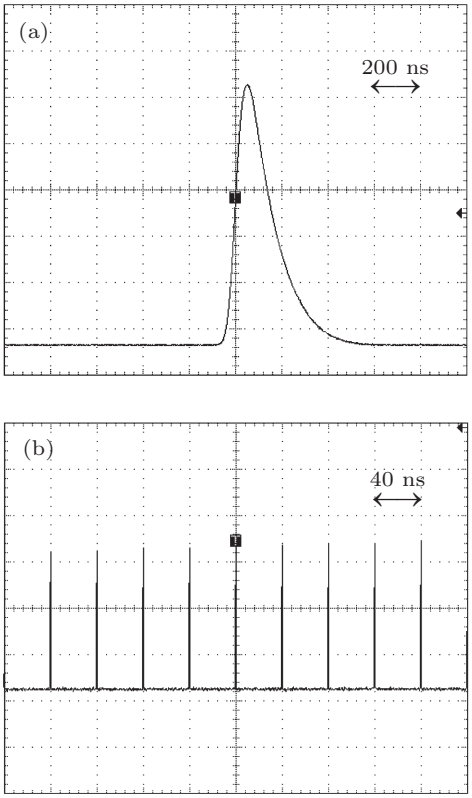


Fig. 5. Oscilloscope traces for 532-nm green laser at an output power of 165 W. (a) Pulse shape and (b) pulse series.

At the diode pump power of 1082 W, the average output power of green laser was measured to be about 160 W in 2.5 h with a time interval of 10 min. The results are presented in Fig. 6. Base on the root mean square error equation $\Delta\bar{P} = \left[\sum_{i=1}^{n}(P_i - \bar{P})^2/n\right]^{1/2}$, the calculated output power fluctuation $\Delta\bar{P}/\bar{P}$ was less than 0.3%. Moreover, the measured pulse to pulse instability was 2%. The good stability of the green laser can be attributed to higher thermal conductivity of the composite ceramic Nd:YAG laser rod and the construction of composite ceramic Nd:YAG rod (with both ends undoped), which can provide the heat sink and decrease thermal stress in the laser rod.

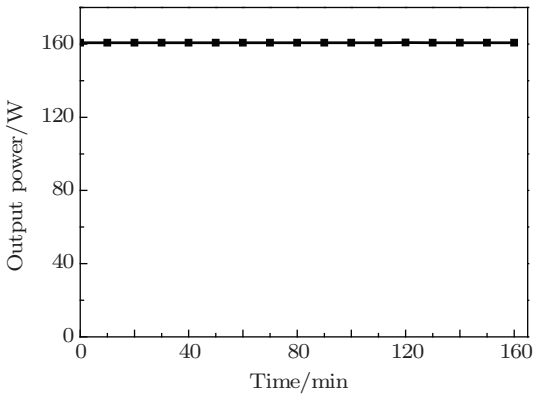


Fig. 6. Stability performance of 160-W green laser based on composite ceramic Nd:YAG crystal.

5. Conclusion

In conclusion, the thermal distribution in transversally pumped composite ceramic Nd:YAG crystal has been numerically analyzed with finite element method. The result showed that the heat inside the rod can be efficiently transferred to the end due to the composite structure compared with the conventional Nd:YAG crystal. In experiment, we have successfully obtained a high-stability 165-W green laser at 532 nm by using diode-side-pumped intracavity-frequency-doubling of double Q-switched composite ceramic Nd:YAG rod laser with HGRT-KTP crystal. The diode-to-green optical conversion efficiency reaches 14.68%. To our knowledge, both the average output power and optical-to-optical conversion efficiency are the highest for this kind of high-power diode-pumped ceramic green laser. The power fluctuation at an average output power of around 160 W was less than 0.3% over 2.5 hours. Such a system with straight plano-concave cavity is an attractive green laser source with advantages of high power, high efficiency, high stability, simple and compact structure.

References

[1] Reich O, Bachmann A, Siebels M, Hofstetter A, Stief C G and Sulser T 2005 *J. Urology* **173** 158

[2] Bandello F, Brancato R and Lattanzio R 1998 *Laser. Med. Sci.* **19** 173

[3] Le Garrec B J, Razé G J, Thro P Y and Gilbert M 1996 *Opt. Lett.* **21** 1990

[4] Chang J J, Dragon E P, Ebbers C A and Bass I L 1998 *Conference on Lasers and Electro-Optics of OSA Technical Digest Series* (vol. 7) (Washington: Optical Society of America) paper CPD-2

[5] Honea E C, Christopher A, Beach R J, Speth J A, Skidmore J A, Emanuel M A and Payne S A 1998 *Opt. Lett.* **23** 1203

[6] Konno S, Kojima T, Fujikawa S and Yasui K 2000 *Opt. Lett.* **25** 105

[7] Yi J, Moon H J and Lee J 2004 *Appl. Opt.* **43** 3732

[8] Gong A C, Bo Y, Bi Y, Sun Z P, Yang X D, Peng Q J, Li H Q, Zhou Y, Li R N, Cui D F and Xu Z Y 2005 *Chin. Phys. Lett.* **22** 125

[9] Xu D G, Yao J Q, Zhang B G, Zhou R, Li E B, Zhao S Y, Ding X, Wen W Q, Niu Y X, Hu J G and Wang P 2005 *Opt. Commun.* **245** 341

[10] Bo Y, Cui Q J, Geng A C, Yang X D, Peng Q J, Lu Y F, Cui D F and Xu Z Y 2007 *Conference on Lasers and Electro-Optics* May 6–11, 2007 Baltimore, USA, paper CTuD4

[11] Dudley D R, Mehl O, Wangm G Y, Allee E S, Pang H Y and Hodgson N 2009 *Proc. SPIE* **7193** 71930

[12] Sharma S K, Mukhopadhyay P K, Singh A, Kandasamy R and Oak S M 2010 *Rev. Sci. Instrum.* **81** 073104

[13] Hajiesmaeilbaigi F, Razzaghi H, Mahdizadeh M, Moghaddam M R A and Ruzbehani M 2011 *Opt. Laser Technol.* **43** 1428

[14] Zhang S, Guo L, Xiong B, Liu Y, Hou W, Lin X and Li J 2011 *Appl. Phys.* B **104** 861

[15] Xu D, Wang Y, Li H, Yao J and Tsang Y H 2007 *Opt. Express* **15** 3991

[16] Zhang Y P, Zhang H Y, Zhong K, Wang P, Li X F and Yao J Q 2009 *Acta Phys. Sin.* **58** 3193 (in Chinese)

[17] Lan R J, Liu H, Wang Z P, Ren Q, Zhang H J, Wang J Y, Yu H H, Lü Y H, Sang Y H and Xu X G 2009 *Acta Phys. Sin.* **58** 7686 (in Chinese)

[18] Kumar G A, Lu J, Kaminskii A A, Ueda K, Yagi H, Yanagitani T and Unnikrishnan N V 2004 *IEEE J. Quantum Electron.* **40** 747

[19] Boulanger B, Fejer M M, Blachman R and Bordui P F 1994 *Appl. Phys. Lett.* **65** 2401

[20] Yao J Q, Yu Y Z, Chen J, Zhang F, Wang P, Wang T and Zhang B G 2001 *Chin. Phys. Lett.* **18** 1356

[21] Lucianetti A, Graf Th, Weber R and Weber H P 2000 *IEEE J. Quantum Electron.* **30** 220

[22] Weber R, Neuenschwander B, Mac Donald M, Roos M B and Weber H P 1998 *IEEE J. Quantum Electron.* **34** 1046